JACS
JOURNAL OF THE AMERICAN CHEMICAL SOCIETY

Article

pubs.acs.org/JACS

Tip-Enhanced Raman Spectroscopy (TERS) for *in Situ* Identification of Indigo and Iron Gall Ink on Paper

Dmitry Kurouski,[†] Stephanie Zaleski,[†] Francesca Casadio,[‡] Richard P. Van Duyne,*[,†] and Nilam C. Shah*[,†]

[†]Department of Chemistry, Northwestern University, 2145 Sheridan Road, Evanston, Illinois United States

[‡]The Art Institute of Chicago, 111 S. Michigan Avenue, Chicago, Illinois United States

Supporting Information

ABSTRACT: Confirmatory, nondestructive, and noninvasive identification of colorants *in situ* is of critical importance for the understanding of historical context and for the long-term preservation of cultural heritage objects. Although there are several established techniques for analyzing cultural heritage materials, there are very few analytical methods that can be used for molecular characterization when very little sample is available, and a minimally invasive approach is required. Tip-enhanced Raman spectroscopy (TERS) is a powerful analytical technique whose key features include high mass sensitivity, high spatial resolution, and precise positioning of the tip. In the current proof-of-concept study we utilized TERS to identify indigo dye and iron gall ink *in situ* on Kinwashi paper. In addition, TERS was used to identify iron gall ink on a historical document with handwritten text dated to the 19th century. We demonstrate that TERS can identify both of these colorants directly on paper. Moreover, vibrational modes from individual components of a complex chemical mixture, iron gall ink, can be identified. To the best of our knowledge, this is the first demonstration of *in situ* TERS for colorants of artistic relevance directly on historical materials. Overall, this work demonstrates the great potential of TERS as an additional spectroscopic tool for minimally invasive compositional characterization of artworks *in situ* and opens exciting new possibilities for cultural heritage research.

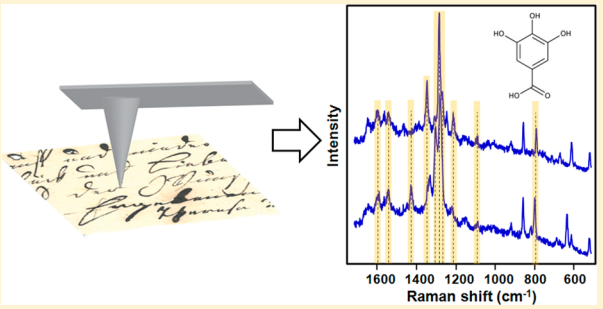

1. INTRODUCTION

The ability to unambiguously identify colorants in artworks and archeological objects is crucial toward understanding a work's historical significance, determining its state of conservation, identifying degradation products, tracing historic trade routes, and supporting conservation. In particular, organic colorants of plant, insect, and synthetic origin are difficult to identify due to their low concentration in artworks, overall poor photostability (leading to further depletion of chromophores available for testing), and high fluorescence when probed with techniques, such as normal Raman spectroscopy.[1] The most well-established means of identifying organic colorants in artworks is high-performance liquid chromatography (HPLC).[2−5] However, HPLC cannot be used when very little sample is available, and a minimally invasive technique is required. UV/Vis spectroscopy is also used to identify dyes such as the anthraquinone red lake pigments.[6] However, absorbance spectra are typically broad and featureless, which substantially complicates definitive pigment identification.[7] Additionally, microspectrofluorimetry has been implemented to differentiate organic colorants by their fluorescence spectra and has been shown to be noninvasive, nondestructive and have micrometer-scale spatial resolution. For example, it was recently demonstrated that *in situ* fluorimetry confirmed the presence of indigo in Renaissance tapestries.[8] However, although this technique is sensitive it is not very specific and cannot differentiate colorants in mixtures.[3,4] FTIR and normal Raman spectroscopy also provide noninvasive and nondestructive detection and identification of various colorants. However, the application of Raman is often limited by the high fluorescence of most of organic dyes, while FTIR suffers from poor sensitivity for colorants incorporated in complex matrices.[9]

In recent years, surface-enhanced Raman spectroscopy (SERS) has become a promising method of organic colorant identification.[10] SERS amplifies the Raman scattering of an analyte due to the interaction of the analyte with a roughened noble metal surface. As a result SERS has extremely high sensitivity down to the single molecule level, requires very little sample, and has the ability to quench fluorescence.[11−14] SERS has successfully provided specific molecular fingerprinting for many cultural heritage applications drastically reducing the amount of sample required compared to HPLC analysis.[10,15−19] However, SERS is currently mostly limited to the identification of a single dye in samples removed from their original objects. In many cases, SERS analysis requires hydrolysis and extraction of the dyestuff, resulting in a loss of important spatial

Received: March 18, 2014

   dx.doi.org/10.1021/ja5027612 | J. Am. Chem. Soc. XXXX, XXX, XXX−XXX

information.[16] Additionally, SERS is not substrate general; the analyte of interest must either be adsorbed onto the enhancing noble metallic nanoparticle substrate or associated near the enhancing substrate with the use of a capture layer. These limitations have recently catalyzed a push toward developing minimally invasive and substrate general SERS-based techniques.[19−24]

Tip-enhanced Raman spectroscopy (TERS) is a powerful technique that combines the sensitivity of SERS and the precise spatial control and resolution of scanning probe microscopy (SPM) via a nanometer-scale noble metal scanning tip.[25,26] Due to this sensitivity, single-molecule detection has been achieved using TERS.[27−29] Two forms of SPM include scanning tunneling microscopy (STM) and atomic force microscopy (AFM). When the scanning tip is irradiated with focused laser excitation, the enhancing region is confined to the apex of the scanning tip, and only molecules within the apex are probed. The probe is placed on top of the surface being analyzed and can easily be withdrawn from the sample's surface after spectral acquisition without concerns of leaving behind any residues, which may be an issue with some of the recently proposed detachable SERS substrates.[20] These capabilities make TERS both minimally invasive and surface general making it a promising technique for analysis of cultural heritage items in cases where very little sample is available and the sample is highly fluorescent. The substrate generality of TERS has already been applied to various problems in biology and surface chemistry such as detecting cytochrome *c* oxidation in mitochondria,[30] DNA,[31] monitoring catalytic reactions,[32] and imaging mixed polymer surfaces[33] and single-walled carbon nanotubes.[34,35] Using TERS to noninvasively identify organic colorants directly from artworks would attest to its strong analytical capability and would provide a new tool for the identification of organic colorants in artworks that cannot otherwise be examined. Herein, we have developed AFM-TERS instrumentation and applied TERS as a novel, minimally invasive, and surface general alternative to SERS in order to identify the colorants indigo and iron gall ink directly on Kinwashi rice paper (K. paper) and on a fragment of historic paper dating to the 19th century

Indigo is a blue dye extracted from the leaves of various *Indigofera* species. It has been used as a colorant since the ancient Egyptian era and gradually spread to the Mediterranean and Europe by Phoenician traders and migrating people. In 1870 A. Bayer synthesized indigo, and by 1913, synthetic indigo almost replaced its natural analogue. In the beginning of the 21st century, indigo was one of the most popular dyes used in textile coloring and painting and remains popular even today.[36]

Iron gall ink was perhaps the most commonly used ink in Western history since it was primarily used as a writing source from the 12th century to the end of the 20th century.[37] It is commonly composed of four main components: galls (gallic or gallotanic acid), vitriol ($FeSO_4$), a polysaccharide binder (such as gum Arabic), and water. When iron gall ink interacts with paper, it penetrates the cellulose fibers and becomes very resistant to smudging, making it an ideal choice for record keeping. In order to increase ink stability and enrich the color, additional ingredients, such as whiskey, vinegar, honey, and logwood were commonly used. The exact formulation of iron gall ink varied based on time period, location, and manufacturer. Thus, identification of specific components in iron gall ink can potentially shed light on the origin of the ink.

Developing TERS instrumentation for the identification of colorants in cultural heritage artifacts is not trivial. One of the most commonly used TERS techniques, STM-TERS, requires the sample to be on conductive surfaces.[38,39] However, most colorants used in cultural heritage objects are applied on substrates, such as paper and natural fibers, or included in complex systems, such as paints and plastics, which are not conductive surfaces. Alternatively, AFM-TERS can analyze both conductive and nonconductive samples. AFM-TERS has successfully been applied to resolve the surface organization of numerous soft biological samples, including DNA, amyloid fibrils, cells membranes, and viruses.[40−43] In order to develop TERS for cultural heritage applications, we built an AFM-TERS instrument in the bottom-illumination configuration, equipped with a 20× dry Nikon objective (Figure 1) for minimally

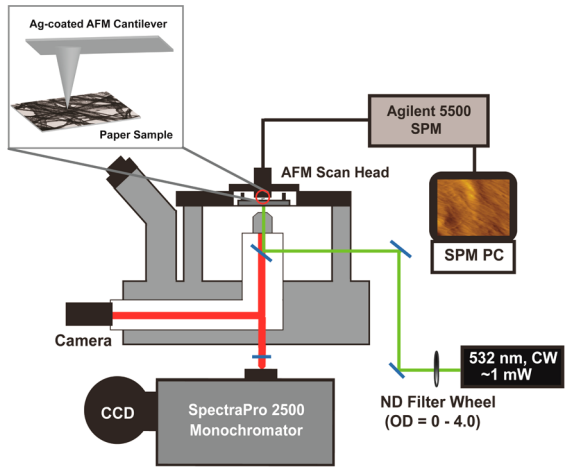

Figure 1. Schematic of home-built AFM-TERS instrument. Inset: Schematic of the interaction between the AFM tip and the sample (photomicrograph of K. paper).

invasive, *in situ* analysis of artworks. This configuration has allowed us to study samples that are either translucent or contain holes or cracks. Using this TERS setup we were able to acquire TER spectra directly from undyed and dyed K. paper and a 19th century historical manuscript using low laser powers (~0.2 mW) and fast acquisition times (3−10 s) avoiding any damage or photodegradation to the dyed paper. In this work, we used dyes that can be identified using normal Raman spectra for comparison of vibrational modes. In future studies, we intend to use TERS for identification of colorants that are highly fluorescent and give no spectra under normal Raman conditions. This proof-of-concept work confirms the analytical potential of TERS as new spectroscopic tool for cultural heritage applications that can identify organic colorants in artworks with high sensitivity, high spatial resolution, and minimal invasiveness.

2. EXPERIMENTAL SECTION

2.1. Materials. Kinwashi paper was purchased from a local art supply store (Blick). Synthetic indigo and gallic acid were purchased from Sigma-Aldrich (St. Louis, MO) and used as received. Iron gall ink solution was received from the Art Institute of Chicago (Enzo brand, iron gall writing ink, Lunalux Art and Design Workshop, Minneapolis, MN). Nanosensors PPP-NCL contact mode AFM cantilevers were purchased from NanoandMore USA, Inc. (Lady's Island, SC). Water was purified using a Millipore Milli-Q system (18 MΩ).

dx.doi.org/10.1021/ja5027612 | J. Am. Chem. Soc. XXXX, XXX, XXX−XXX

2.2. Sample Preparation. Glass microscope coverslips (Fisher Scientific) were pretreated in two steps: (1) piranha etch, 3:1 H_2SO_4/30% H_2O_2 at 80 °C for 1 h, to clean the substrate, and (2) base treatment, 5:1:1 H_2O/NH_4OH/30% H_2O_2 with sonication for 1 h, to render the surface hydrophilic. For reference spectra, 8 nm of Au were deposited on cleaned glass coverslips using PVD-75 Thermal Evaporator (Kurt J. Lesker) at a rate of 1 Å/s. Synthetic indigo solutions were prepared in Milli-Q water, and 1 M NaOH was added to the solution dropwise to obtain a pH of 10−11. Au films were incubated in a 1 mM indigo solution for 30 min and dried in air at room temperature. Reference paper samples were prepared by submerging a piece of K. paper for ∼5 min in separate solutions of: (1) 0.5 mM indigo solution and (2) an iron gall ink solution. The two individual paper samples were then dried in air at room temperature. K. paper was found to be translucent which allowed us to acquire TER spectra in a bottom-illumination configuration. A representative photograph and micrograph of K. paper is shown in Figure S1. AFM images were taken of paper exposed to pH 10−11 for ∼5 min to ensure no paper degradation occurred (Figure S2). TERS probes were prepared by electron beam deposition (AXXIS, Kurt J. Lesker) of 20−40 nm Ag at a rate of 0.5 Å/s onto contact mode AFM cantilevers.

2.3. TERS Instrumentation. All TER spectra were acquired on a home-built microscope system. A 532 nm CW laser (Spectra Physics, Mountain View, CA) was used as the excitation source, and the power was adjusted with a neutral density filter wheel (ThorLabs, Newton, NJ). Laser powers at the samples were 0.16 mW for K. paper and 0.36 mW for 19th century historical paper. The light source was directed into the back port of an inverted Nikon TE-2000U microscope, reflected off of a 10/90 beam splitter, and directed upward into a 0.45 numerical aperture (NA) 20× dry Nikon objective. An Agilent/Molecular Imaging PicoPlus AFM was mounted on a Renishaw motorized stage for AFM imaging and XY laser positioning, respectively. The sample of interest was clipped to an Agilent PicoPlus AFM sample holder. For K. paper, the paper sample was approached with an AFM tip and the objective focus was adjusted to view the tip apex (Figure S3) using a CCD camera (UNIQ Vision, Inc., Santa Clara, CA) attached to the microscope. The 532 nm CW laser light was then visually focused on the tip apex using a Renishaw XY motorized microscope stage controlled by Prior ProScan II. For historical paper, a single fiber near the circumference of one of the cracks was approached with the Ag AFM tip. Precise alignment of the laser on the tip apex was monitored by maximizing the intensity of the Si optical phonon mode at 521 cm^{-1} from the AFM cantilever. The AFM scanner implemented an IR diode feedback laser, which prevents spectral interference in TERS measurements. The scattered light is collected through the objective, passed through a 532 nm long-pass filter (Semrock, LP03−532RS-25) to filter Rayleigh light, and directed to a confocal Raman spectrometer (Princeton Instruments, SP2500i) equipped with a 1200 groove/mm grating and a slit entrance set to 100 μm. The dispersed light is then sent to a liquid nitrogen-cooled PI-Acton Spec-10 CCD for spectral acquisition.

2.4. Normal Raman (NR) Spectroscopy. NR spectra were collected on an inverted microscope (Nikon TE-300) with 20× dry Nikon objective (NA = 0.45). A diode pumped solid-state laser (Spectra-Physics Millenia) was used for 532 nm excitation. It was also utilized to drive the tunable Ti:sapphire oscillator to generate 785 nm light. The signal was collected in a backscattering geometry and directed to a confocal Raman spectrometer (Princeton Instruments, SP2500i) equipped with a 1200 groove/mm grating (532 nm excitation) or 600 groove/mm grating (785 nm excitation) and a slit entrance set to 100 μm. Prior to entering the spectrograph Rayleigh scattering was filtered with a long-pass filter (Semrock, LP03−532RS-25 (532 nm excitation) or LP03-785RS-25 (785 nm excitation)). The dispersed light is then sent to a liquid nitrogen-cooled CCD (Action300i, Spec-10 400B).

2.5. Spectral Processing. For all spectra shown, the raw intensity counts were divided by the power and acquisition time to normalize the spectral intensity, such that the intensity is reported in the units of analog to digital conversion units or ADU mW^{-1} s^{-1}. All data was processed using GRAMS/AI 7.0 (Thermo Galactic, Salem, NH).

3. RESULTS AND DISCUSSION

3.1. TERS Measurements of Indigo on Kinwashi Rice Paper. Using TERS we analyzed K. paper dyed with 0.5 mM indigo. Figure 2 shows the TER spectra of indigo on K. paper,

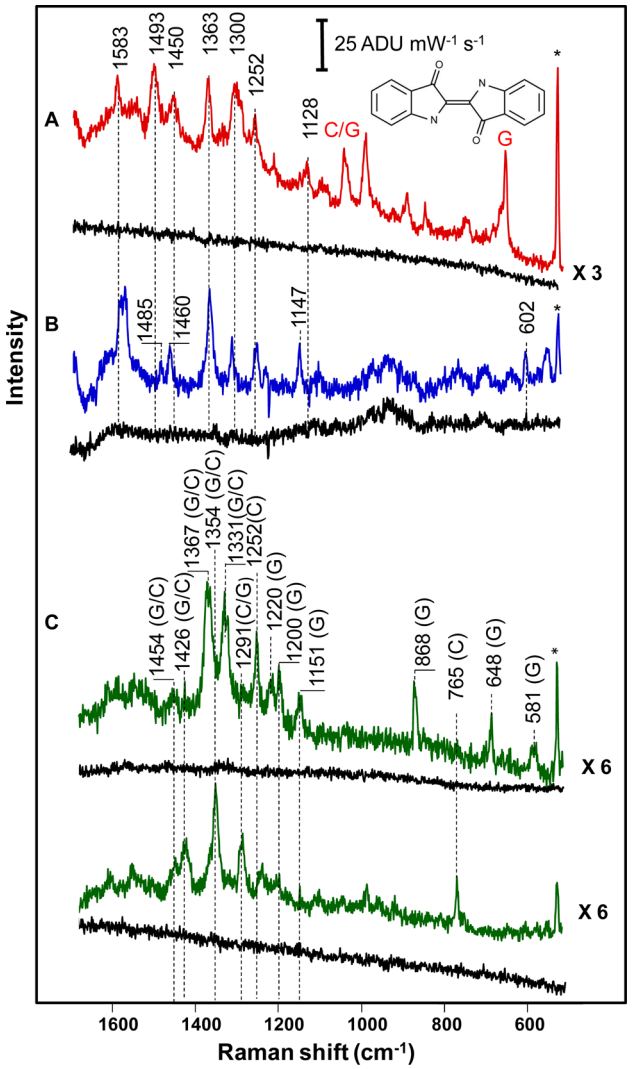

Figure 2. TER spectra of (A) K. paper dyed with 0.5 mM indigo engaged (red) and retracted (black); (B) indigo on gold film engaged (blue) and retracted (black); representative TERS spectra of (C) undyed Kinwashi paper engaged (green) and retracted (black). The asterisk (*) indicates the peak at 521 cm^{-1} that results from silicon on the AFM tip. TER spectra acquired using λ_{ex} = 532 nm; t_{acq} ≈ 10 s (A), 120 s (B), 3 s (C); P_{ex} ≈ 0.16 mW (A, C) and 0.3 mW (B). Peaks corresponding to the vibrational modes of both cellulose and glucose and just glucose are marked with "C/G" and "G", respectively.

indigo on 8 nm Au film, and undyed K. paper with the tip engaged and retracted. The engaged spectra show the enhancement of signal due to TERS. The retracted spectra demonstrate that no far-field signal is observed indicating that the engaged signal is from TERS and not from SERS or Raman.

We observed peaks corresponding to both indigo (Figure 2B) and K. paper (Figure 2C). We found that four bands at 1583, 1363, 1300, and 1252 cm^{-1} observed in the TER spectrum of indigo dyed K. paper (Figure 2A) match well with the corresponding bands in the TER spectrum of indigo on Au film (Figure 2B). Furthermore, three bands centered at 1493,

dx.doi.org/10.1021/ja5027612 | J. Am. Chem. Soc. XXXX, XXX, XXX−XXX

1450, and 1128 in the TER spectrum of indigo on K. paper were shifted from the corresponding bands in the TER spectra of indigo on Au film (1485, 1460 and 1147). Finally, we did not observe a band at 602 cm^{-1} (the N−H bending) mode in the TER spectrum of indigo on the paper which is present in the TER spectra of indigo on Au film. Additional bands were also observed at 1033, 986, 868, and 648 cm^{-1}. In order to understand the origin of these additional bands we acquired several spectra from various areas on undyed K. paper. TER spectra from undyed K. paper, which is primarily composed of cellulose, are shown in Figure 2C, and the corresponding peaks are shown in Table 1. It was found that almost all the observed

Table 1. Vibrational Bands of TERS Spectra Acquired from Undyed K. Paper and Corresponding Vibrational Modes of Cellulose and Glucose (Normal Raman; refs 44, 45, and 55)[a]

TERS of undyed paper (cm^{-1})	normal Raman of cellulose (cm^{-1})[44,45,55]	normal Raman of glucose (cm^{-1})[44,45,55]	assignment[b,44,45,55]
1454	1454	1452	$\delta(CH_2)$; δ(COH)
1426	1432	1433	$\delta(CH_2)$
1367	1377	1375	δ(CH); δ(OH)
1354	1359	1346	CH def; δ(COH)
1331	1337	1335	$\delta(CH_2)$; OH def
1291	1293	1298	$\delta(CH_2)$
1252	1249	–	γ(COH)
1220	–	1224	$\delta(CH_2)$
1200	–	1206	δ(COH); δ(CCH)
1151	1153	1153	ν(CC)rg. br. a
1033*	1026	1022	δ(COH)
868	–	859	δ(CH); (CH_2)
765	765	–	ν(C−C)
648	–	648	
–	–	601	skeletal modes
581	–	581	

[a]Asterisk (*) indicates bands that only appear in indigo dyed K. paper. [b]rg = ring; br = breath; a = asymmetric; ν = stretch; δ = bend; γ = out-of-plane deformation.

vibrational bands in K. paper originate either from cellulose or its monomer, glucose. Vibrational modes centered at 1454, 1426, 1367, 1354, 1331, and 1291 cm^{-1} can be assigned to the vibrational modes of both cellulose and glucose based on literature values.[44,45] For example, the band at 1426 cm^{-1} corresponds to the methylene bending vibration of the sugar ring.[46] Additionally, bands centered at 1252 and 765 cm^{-1} can be assigned to cellulose and bands centered at 1220, 1200, 1151, 868, 648, and 581 cm^{-1} to glucose.[45] Peak positions in the acquired TERS spectra of undyed paper are shifted 2−9 cm^{-1} compared to the corresponding peaks in the normal Raman spectra of cellulose and glucose. This shift in peak position can be due to molecule−metal interaction effects and possible differences in spectrometer calibrations when comparing to literature values.[47,48]

The ability of TERS to detect chemical components of paper with high sensitivity makes it challenging to assign some vibrational modes of indigo. For example, we found that the vibrational modes of indigo centered at 1363 and 1252 cm^{-1} overlap with the 1367 cm^{-1} peak, attributed to cellulose and glucose, and the 1252 cm^{-1} peak, attributed to cellulose, found in undyed K. paper. The vibrational mode at 1033 from indigo dyed K. paper is similar to a band found in glucose, however, this peak is not observed in undyed K. paper. Previously theoretical predictions based on minimal steric difference (MDT) calculations suggested that vat dyes such as indigo experience steric, hydrophobic, and electrostatic effects and hydrogen bonding upon interactions with cellulose.[49] The observed shifts and additional and missing peaks may be a result of these types of dye-interactions when K. paper is dyed with indigo. For example, it has been shown in previous work that the NH out-of-plane bending mode disappears, and the NH in-plane bending mode is reduced in intensity when the spectra of free indigo dye and indigo dye complexed to a clay matrix are compared.[50] Experiments and theoretical work are currently being conducted to better understand dye−cellulose interactions and unambiguously assign all of the bands. Nevertheless, these proof-of-concept experiments demonstrate for the first time that it is possible to obtain high signal-to-noise spectra of dyes on paper substrates with TERS using low laser powers and short acquisition times.

To elucidate TERS spectral variations across the substrate and to demonstrate that indigo can be unambiguously detected on K. paper, we acquired 100 spectra from different locations on K. paper dyed with indigo, and several representative spectra are shown in Figure 3. There are small spectral variations that are very likely due to the chemical heterogeneity of K. paper at

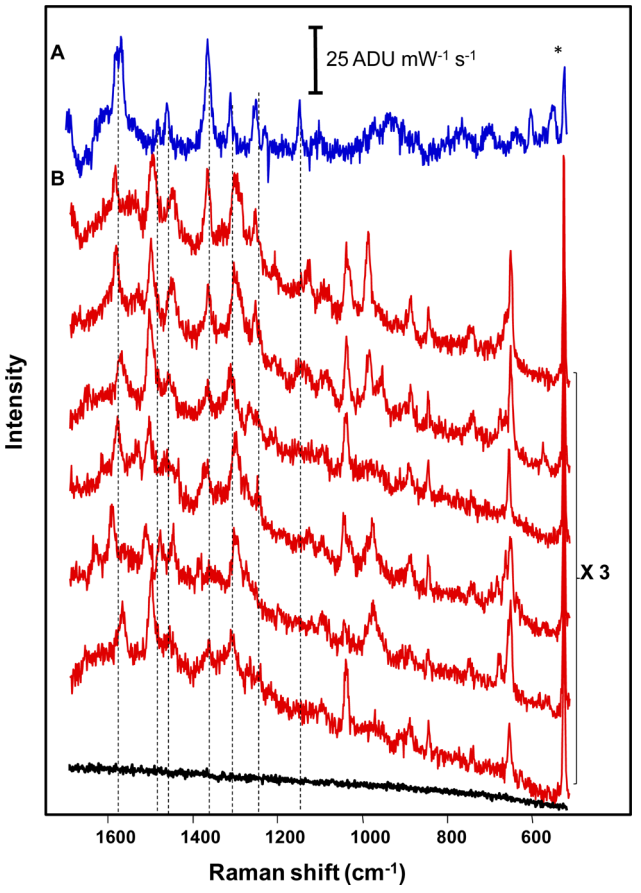

Figure 3. TER spectra of (A) indigo on gold film and (B) representative TER spectra, taken at different locations, of K. paper dyed with 0.5 mM indigo engaged (red) and retracted (black). The asterisk (*) indicates the peak at 521 cm^{-1} that results from silicon on the AFM tip. TER spectra acquired using λ_{ex} = 532 nm; $t_{acq} \approx$ (A) 120 s and (B) 10 s; $P_{ex} \approx$ 0.16−0.18 mW.

dx.doi.org/10.1021/ja5027612 | J. Am. Chem. Soc. XXXX, XXX, XXX−XXX

the microscopic level. The vibrational bands originating from indigo undergo ±7 cm^{-1} shifts from one spectrum to another. These small shifts are consistent with similar vibrational band shifts observed in previously reported TERS spectra of small molecules.[51−53]

In general, unambiguous identification of all vibrational modes of TERS spectra acquired from heterogeneous samples is challenging. This is partly due to the fact that the exact chemical composition of heterogeneous samples is commonly unknown. Furthermore, different molecules may exhibit the same vibrational modes such as those originating from aliphatic (CH_2 and CH_3) or aromatic (benzene) groups. This has been previously observed in TERS spectra of complex heterogeneous biological samples such as proteins, amyloid fibrils and cells.[43,54] Nevertheless, our experiments demonstrate that it is possible to obtain high signal-to-noise spectra of indigo using TERS. While fluctuations in peak intensities and positions exist at different tip locations, an ensemble-averaged spectrum can be approached by averaging individual acquisitions. The ensemble-averaged spectrum is an alternative way to show vibrational modes that are most prominent in the heterogeneous substrate. We averaged 10 TER spectra acquired from K. paper dyed with indigo (Figure S4A). Some band deviations, primarily in the lower frequency region (cellulose and glucose peaks), can be noted between an individual TER spectrum and the average TER spectrum. Nevertheless, all bands that originate from indigo remain in the average TER spectrum.

3.2. TERS Measurements of Iron Gall Ink on Kinwashi Rice Paper. We also used TERS to detect a more complex dye, iron gall ink. The identification of individual components of iron gall ink, as well as its tannin content, on paper documents is challenging because very little material is contained in the traced lines.[56] Moreover, very little material is available for sampling from the majority of historical documents. Currently, identification of iron gall ink in underdrawings and manuscripts is primarily done using X-ray fluorescence (XRF) as well as inductively coupled plasma (ICP) spectroscopy and is based on the detection of metallic ions. However, contamination of paper can result in the presence of various metal ions including iron, copper, zinc, and manganese. This makes it difficult to determine if the metallic elements actually originate from the ink.[57] In addition, ICP is destructive and as a result its application is substantially limited in conservation science.[58] Furthermore, both of these techniques are unable to provide information about the organic colorants of the ink.[37] While Raman spectroscopy and terahertz spectroscopy have been used to characterize iron gall inks, they each have their own limitations. Specifically, Raman spectroscopy is often limited by the high fluorescence of most organic dyes, degradation products, or the substrate containing the dyes. On the other hand, terahertz spectroscopy requires a large sample size which is limiting in cultural heritage applications when very little sample is available.[10,59] Thus, we investigated the use of TERS for analysis of iron gall ink on K. paper.

We observed a total of 10 peaks in the TER spectrum of iron gall ink on K. paper centered at 1460, 1433, 1395, 1333, 1275, 1197, 1170, 780, 644, and 562 cm^{-1} (Figure 4). The spectrum was compared to the normal Raman spectra of iron gall ink (Figure 4C) and gallic acid, the primary component of iron gall ink (Figure 4B). The normal Raman spectra were acquired using 785 nm excitation due to the high fluorescence of the ink at 532 nm excitation (Figure S5). The vibrational bands centered at 1395, 1275, 780, and 562 cm^{-1} can be attributed to

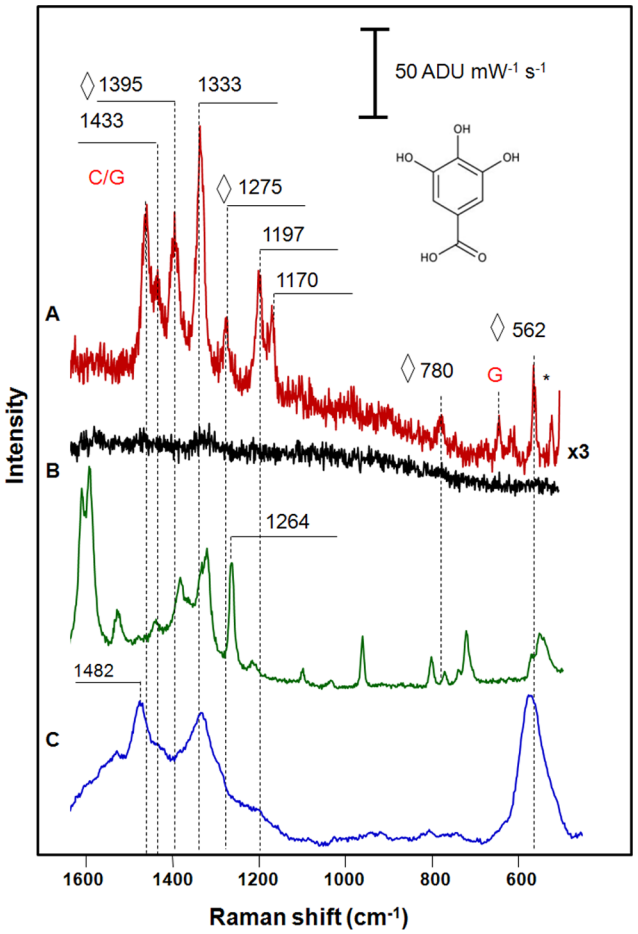

Figure 4. TER spectra of (A) K. paper dyed with iron gall ink engaged (red) and retracted (black). The asterisk (*) indicates the peak at 521 cm^{-1} that results from silicon on the AFM tip. TER spectra acquired using λ_{ex} = 532 nm; t_{acq} = 4 s; P_{ex} ≈ 0.25 mW. Normal Raman spectra of (B) gallic acid powder and (C) iron gall ink in solution. Raman spectra were acquired using λ_{ex} = 785 nm; t_{acq} = 10 and 60 s, respectively; and P_{ex} ≈ 1 mW. Peaks corresponding to gallic acid in the TER spectra are marked with ◊. Peaks corresponding to the vibrational modes of both cellulose and glucose and just glucose are marked with "C/G" and "G", respectively.

gallic acid.[60] Two of the observed vibrational modes centered at 1460 and 644 cm^{-1} can be attributed to K. paper (Figure 2). The peaks centered at 1433, 1333, and 1197 cm^{-1} are present in both K. paper and iron gall ink. Furthermore, we did not observe a peak at 1482 cm^{-1} in the TER spectrum collected from the iron gall ink on K. paper, while this band was observed in the normal Raman spectrum acquired at 785 nm. There is also a peak present at 1170 cm^{-1} which cannot be assigned. Nevertheless, our experiments demonstrate that it is possible to obtain high signal-to-noise spectra of iron gall ink using TERS. While fluctuations in peak intensities and positions exist at different tip locations, the ensemble-averaged spectrum (obtained from a total of 6 spectra) demonstrates that several relevant iron gall ink peaks are present (1395, 1333, 1275, 780 and 562) (see Figure S4C). Nevertheless, the ensemble-averaged spectrum demonstrates that TERS is able to detect the individual component, gallic acid, in the complex mixture of iron gall ink, which cannot be revealed by normal Raman spectroscopy even when using higher laser powers and longer acquisition times (Figure 4).[56]

dx.doi.org/10.1021/ja5027612 | J. Am. Chem. Soc. XXXX, XXX, XXX−XXX

The spectra demonstrate that not all vibrational modes of individual components are simultaneously observed in the acquired TERS spectra. This phenomenon was previously observed for amino acids,[53,61] peptides and proteins,[43,62] calcium oxalate monohydrate crystals,[63] and DNA.[64] There is an ongoing discussion about factors that can contribute to this, such as molecule−substrate and molecule−tip interactions as well as molecule orientation relative to incident laser light.[25,43,47,48] Theoretical studies are underway to gain a deeper understanding of this phenomenon.

3.3. TERS of 19th Century Historical Paper. We also investigated the application of TERS for analysis of a letter from the 19th century written on paper. Iron gall ink degradation causes corrosion of paper resulting in cracks that are visible on the surface of the historical paper (Figure 5D). In our experiment an Ag-coated AFM tip was positioned on a single fiber of paper near the circumference of one of the cracks, as shown in Figure 5D,E (red arrows), and TER spectra were acquired. Two representative TER spectra (of 28 total spectra) are shown in Figure 5A and the ensemble-averaged TER spectrum is shown in Figure S4D.

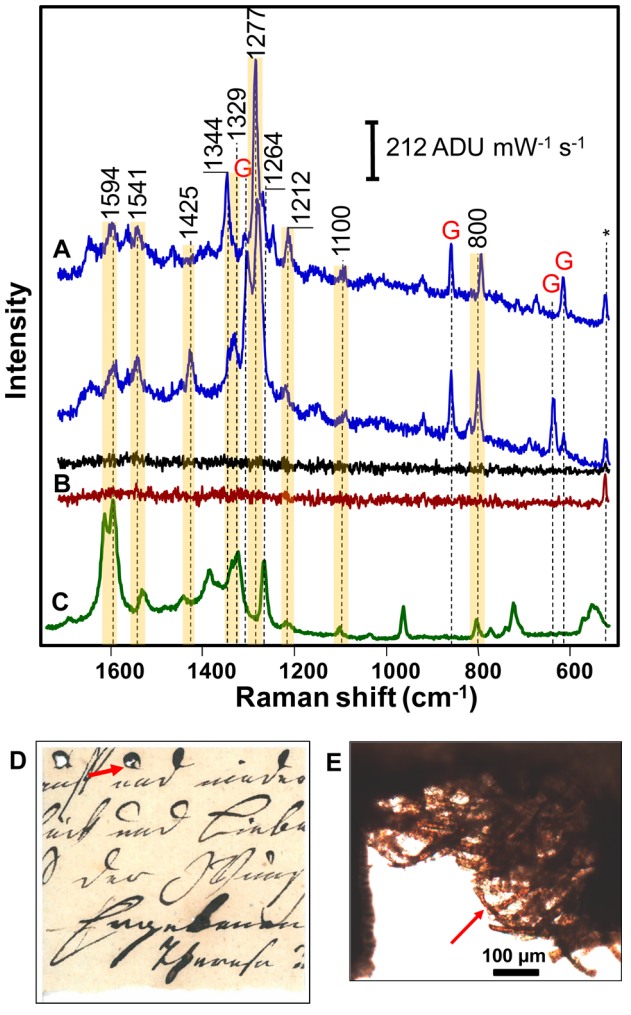

Figure 5. TER spectra of (A) iron gall ink spot on 19th century historical paper engaged (blue) and retracted (black). TER spectrum of (B) the AFM Ag-coated tip removed from the fiber immediately after data acquisition. Normal Raman spectrum of (C) gallic acid powder. Fragment of 19th century letter (D) and a micrograph of the paper crack (E). Red arrow indicates the spot where the AFM Ag-coated tip was positioned. Peaks corresponding to the vibrational modes of glucose are marked by "G". The asterisk (*) indicates the peak at 521 cm^{-1} which results from silicon on the AFM tip. TER spectra acquired using λ_{ex} = 532 nm; t_{acq} = 4 s; $P_{ex} \approx 0.36$ mW. Normal Raman spectrum acquired using λ_{ex} = 785 nm; t_{acq} = 10 s; $P_{ex} \approx 1$ mW.

The TER spectra demonstrate that it is possible to get high signal-to-noise ratio spectra of ink on historical paper from the 19th century. We found that the TER spectra have vibrational modes corresponding to gallic acid and glucose. Specifically, vibrational modes centered at 1594, 1541, 1425, 1344, 1329, 1277, 1264, 1212, 1100, and 800 cm^{-1} originate from gallic acid (Table 2). The peaks centered at 1425, 1344, and 1329 cm^{-1} also overlap with glucose and cellulose peaks. The vibrational modes at 1300, 855, 634, and 613 cm^{-1} (marked with G) correspond to Raman bands of glucose, the monomer of cellulose (Table 1).

Table 2. Vibrational Frequencies of Gallic Acid (normal Raman) and Corresponding Peaks of Iron Gall ink on K. Paper and 19th Century Historical Paper (TERS)

gallic acid (normal Raman), cm^{-1}	iron gall ink on K. rice paper (TERS), cm^{-1}	iron gall ink on paper manuscript dated to 19th century (TERS), cm^{-1}	assignment[b,65]
1611	–	–	ν(CC), γrg
1594	–	1594	ν(CC)
1530	–	1541	
1441	1433	1425	γ(CC)rg
1384	1395	–	
1336	1333	1329; 1344	
1266	1275	1264; 1277	γ(C═O)
1216	1197	1212	β(C═O)
1100	–	1100	β(OH)
961	–	–	ν(CO)
801	–	800	γ(CH)
770	780	–	ν(CC), β(C−O)
721	–	–	τ(C−O)
567	562	–	γ(CO)
548	–	–	βrg

[b]rg = ring; ν = stretch; β = in-plane deformation; γ = out-of-plane deformation; τ = torsion.

As shown in Table 2, the 1266 cm^{-1} mode only appears in the normal Raman spectrum of gallic acid, whereas the 1275 cm^{-1} mode only appears in the spectrum of K. paper dyed with gallic acid. However, we observe both vibrational modes (1264 and 1277 cm^{-1}) in the historical 19th century paper sample. These two peaks may be attributed to gallic acid that are either bound or unbound to cellulose. We observe a similar pattern for the 1329 and 1344 cm^{-1} modes. In both cases, we found that peak positions in the acquired TERS spectra are shifted 2−9 cm^{-1} compared to the corresponding peaks in the normal Raman spectra. The observation of both vibrational modes may be potentially attributed to the degradation of iron gall ink in the 19th century paper sample. Additionally, spectral shifts and peak doubling can result from molecule−metal interaction effects and incident light polarization.[25,43,47,48]

Additionally, some modes are observed only in K. paper or in historical paper. The chemical composition of K. paper and historical paper is not known. Since the composition of the two types of paper may be different, the spectral differences may be a result of distinct interactions of gallic acid with different

dx.doi.org/10.1021/ja5027612 | J. Am. Chem. Soc. XXXX, XXX, XXX−XXX

components in K. paper and historical paper, such as hemicellulose and lignin. Additional experimental and theoretical work is currently being conducted to better understand gallic acid−cellulose interactions in different types of paper, which will allow us to fully understand the presence and absence of vibrational bands in the TER spectra.

Immediately after TERS spectral acquisition the tip was moved away from the paper fiber, and laser light was focused on its apex to acquire a spectrum of the tip. One peak was present centered at 521 cm^{-1} that is due to the silicon in the tip (Figure 5B). No other peaks are present indicating that molecules are not transferred to the tip from the historic paper and contamination does not occur. These experiments demonstrate that TERS allows for minimally invasive and nondestructive identification of iron gall ink on real historical documents, such as handwritten manuscripts. Moreover, nanometer length of a single paper fiber is enough to acquire high signal-to-noise spectra.

4. CONCLUSIONS

This work is the first proof-of-concept demonstration of TERS for identification of cultural heritage colorants such as indigo and iron gall ink *in situ* on dyed paper including both reference and historic samples. This approach is ideal for cultural heritage research because it can detect dyes at low concentrations using low laser powers and short acquisition times with good signal-to-noise spectra and high spatial resolution. Furthermore, TERS is a minimally invasive technique, and we have shown that dyes are not transferred to the tip after the tip is retracted. The identification of iron gall ink demonstrates that very detailed spectra can be obtained using TERS compared to normal Raman spectroscopy. The experiments also demonstrate that additional peaks are present in spectra obtained from dyed paper possibly due to dye−paper interactions. Theoretical studies are currently underway to fully understand the origin of these peaks and assign all of the vibrational modes. In addition, we are in the process of building a side-illumination AFM-TERS setup which will allow us to study opaque objects, opening up even greater possibilities for using TERS on a variety of media for cultural heritage analysis. Such future developments could potentially open up exciting opportunities for the nanoscale mapping of organic constituents of works of art.

■ ASSOCIATED CONTENT

Supporting Information

Photograph, micrograph and AFM images are shown in Figures S1-S3. Ensemble-averaged TER spectra are shown in Figure S4. Normal Raman spectra of iron gall ink on a paper manuscript dated to the 19th century are shown in Figure S5. This material is available free of charge via the Internet at http://pubs.acs.org.

■ AUTHOR INFORMATION

Corresponding Authors

vanduyne@northwestern.edu
nilamshah2010@u.northwestern.edu

Notes

The authors declare no competing financial interest.

■ ACKNOWLEDGMENTS

Scientific research at the Art Institute of Chicago is supported by the Andrew W. Mellon and Grainger Foundations. Harriet Stratis is gratefully acknowledged for providing the historic sample of 19th century paper with iron gall ink writings. Conservation science research at the Art Institute of Chicago and Northwestern University is made possible by generous grants from the National Science Foundation (Grants CHE-1041812, CHE-1152547, and CHE-0802913).

■ REFERENCES

(1) Berrie, B. H. *Annu. Rev. Anal. Chem.* **2012**, *5*, 441.
(2) Rosenberg, E. *Anal. Bioanal. Chem.* **2008**, *391*, 33.
(3) Serrano, A.; Sousa, M. M.; Hallett, J.; Lopes, J. A.; Olivera, M. C. *Anal. Bioanal. Chem.* **2011**, *401*, 735.
(4) Degano, I.; Ribechini, E.; Modugno, F.; Colombini, M. P. *Appl. Spectrosc. Rev.* **2009**, *44*, 363.
(5) Karapanagiotis, L.; Valianou, L.; Daniilia, S.; Chryssoulakis, Y. *J. Cult. Herit.* **2007**, *8*, 294.
(6) Montazer, M.; Parvinzadeh. *J. Appl. Polym. Sci.* **2004**, *93*, 2704.
(7) Miliani, C.; Rosi, F.; Brunetti, B. G.; Sgamellotti, A. *Acc. Chem. Res.* **2010**, *43*, 728.
(8) Clementi, C.; Miliani, C.; Romani, A.; Santamaria, U.; Morresi, F.; Mlynarska, K.; Favaro, G. *Spectrochim. Acta* **2009**, *71*, 2057.
(9) Prati, S.; Joseph, E.; Sciutto, G.; Mazzeo, R. *Acc. Chem. Res.* **2010**, *43*, 792.
(10) Casadio, F.; Leona, M.; Lombardi John, R.; Van Duyne, R. P. *Acc. Chem. Res.* **2010**, *43*, 782.
(11) Zrimsek, A.; Henry, A.-I.; Van Duyne, R. P. *J. Phys. Chem. Lett.* **2013**, *4*, 3206.
(12) Le Ru, E. C.; Meyer, M.; Etchegoin, P. G. *J. Phys. Chem. B* **2006**, *110*, 1944.
(13) Stiles, P. L.; Dieringer, J. A.; Shah, N. C.; Van Duyne, R. P. *Annu. Rev. Anal. Chem.* **2008**, *1*, 601.
(14) Dieringer, J. A.; Lettan, R. B., II; Scheidt, K. A.; Van Duyne, R. P. *J. Am. Chem. Soc.* **2007**, *129*, 16249.
(15) Pozzi, F.; Lombardi, J. R.; Bruni, S.; Leona, M. *Anal. Chem.* **2012**, *84*, 3751.
(16) Leona, M. *Proc. Nat. Acad. Sci. U. S. A.* **2009**, *106*, 14757.
(17) Brosseau, C. L.; Casadio, F.; Van Duyne, R. P. *J. Raman. Spectrosc.* **2011**, *42*, 1305.
(18) Brosseau, C. L.; Gambardella, A.; Casadio, F.; Grzywacz, C. M.; Wouters, J.; Van Duyne, R. P. *Anal. Chem.* **2009**, *81*, 3056.
(19) Idone, A.; Gulmini, M.; Henry, A. I.; Casadio, F.; Chang, L.; Appolonia, L.; Van Duyne, R. P.; Shah, N. C. *Analyst* **2013**, *138*, 5895.
(20) Leona, M.; Decuzzi, P.; Kubic, T. A.; Gates, G.; Lombardi, J. R. *Anal. Chem.* **2011**, *83*, 3990.
(21) Ringe, E.; Sharma, B.; Henry, A. I.; Marks, L. D.; Van Duyne, R. P. *Phys. Chem. Chem. Phys.* **2013**, *15*, 4110.
(22) Brosseau, C. L.; Rayner, K. S.; Casadio, F.; Grzywacz, C. M.; Van Duyne, R. P. *Anal. Chem.* **2009**, *81*, 7443.
(23) Jurasekova, Z.; del Puerto, E.; Bruno, G.; Garcia-Ramos, J. V.; Sanchez-Cortes, S.; Domingo, C. *J. Raman Spectrosc.* **2010**, *41*, 1455.
(24) Kleinman, S. L.; Frontiera, R. R.; Henry, A. I.; Dieringer, J. A.; Van Duyne, R. P. *Phys. Chem. Chem. Phys.* **2013**, *15*, 21.
(25) Schmid, T.; Opilik, L.; Blum, C.; Zenobi, R. *Angew. Chem., Int. Ed.* **2013**, *52*, 5940.
(26) Klingsporn, J. M.; Jiang, N.; Pozzi, E. A.; Sonntag, M. D.; Chulhai, D.; Seideman, T.; Jensen, L.; Hersam, M. C.; Van Duyne, R. P. *J. Am. Chem. Soc.* **2014**, *136*, 3881.
(27) Sonntag, M. D.; Klingsporn, J. M.; Garibay, L. K.; Roberts, J. M.; Dieringer, J. A.; Seideman, T.; Scheidt, K. A.; Jensen, L.; Schatz, G. C.; Van Duyne, R. P. *J. Phys. Chem. C* **2012**, *116*, 478.
(28) Zhang, R.; Zhang, Y.; Dong, Z. C.; Jiang, S.; Zhang, C.; Chen, L. G.; Zhang, L.; Liao, Y.; Aizpurua, J.; Luo, Y.; Yang, J. L.; Hou, J. G. *Nature* **2013**, *498*, 82.
(29) Steidtner, J.; Pettinger, B. *Phys. Rev. Lett.* **2008**, *100*, 236101.
(30) Bohme, R.; Mkandawire, M.; Krause-Buchholz, U.; Rosch, P.; Rodel, G.; Popp, J.; Deckert, V. *Chem. Commun.* **2011**, *47*, 11453.

(31) Najjar, S.; Talaga, D.; Schue, T.; Coffinier, Y.; Szunerits, S.; Boukherroub, R.; Servant, L.; Rodriguez, V.; Bonhommeau, S. *J. Phys. Chem. C* **2014**, *118*, 1174.
(32) van SchrojensteinLantman, E. M.; Deckert-Gaudig, T.; Mank, A. J.; Deckert, V.; Weckhuysen, B. M. *Nat. Nanotechnol.* **2012**, *7*, 583.
(33) Yeo, B. S.; Amstad, E.; Schmid, T.; Stadler, J.; Zenobi, R. *Small* **2009**, *5*, 952.
(34) Hartschuh, A.; Sánchez, E.; Xie, X.; Novotny, L. *Phys. Rev. Lett.* **2003**, *90*, 1787.
(35) Chen, C.; Hayazawa, N.; Kawata, S. *Nat. Commun.* **2014**, *5*, 3312.
(36) Schweppe, H. In *Artists' Pigments: A Handbook of Their History and Characteristics*; Fitzhugh, E. W., Ed.; Oxford University Press: Oxford, 1997; Vol. 3.
(37) Bomford, D. *Art in the Making: Underdrawings in Renaissance Paintings*; Yale University Press: New Haven, CT, 2002.
(38) Jiang, N.; Foley, E. T.; Klingsporn, J. M.; Sonntag, M. D.; Valley, N. A.; Dieringer, J. A.; Seideman, T.; Schatz, G. C.; Hersam, M. C.; Van Duyne, R. P. *Nano Lett.* **2012**, *12*, 5061.
(39) Stadler, J.; Schmid, T.; Zenobi, R. *Nanoscale* **2012**, *4*, 1856.
(40) Richter, M.; Hedegaard, M.; Deckert-Gaudig, T.; Lampen, P.; Deckert, V. *Small* **2011**, *7*, 209.
(41) Kurouski, D.; Deckert-Gaudig, T.; Deckert, V.; Lednev, I. K. *J. Am. Chem. Soc.* **2012**, *134*, 13323.
(42) Zhang, M.; Wang, J.; Tian, Q. *Opt. Express* **2014**, *21*, 9414.
(43) Kurouski, D.; Postiglione, T.; Deckert-Gaudig, T.; Deckert, V.; Lednev, I. K. *Analyst* **2013**, *138*, 1665.
(44) Edwards, H. G. M.; Farwell, D. W.; Webster, D. *Spectrochim. Acta, Part A* **1997**, *53*, 2383.
(45) Walton, A. *Biopolymers*; Academic Press: New York, 1973.
(46) Ruiz-Chica, A. J.; Medina, M. A.; Sanchez-Jimenez, F.; Ramirez, F. J. *J. Raman Spectrosc.* **2004**, *35*, 93.
(47) Etchegoin, P. G.; Le Ru, E. C. In *Surface Enhanced Raman Spectroscopy: Analytical, Biophysical and Life Science Applications*; Schlücker, S., Ed.; Wiley: New York, 2011.
(48) Blum, C.; Opilik, L.; Atkin, J. M.; Braun, K.; Kammer, S. B.; Kravtsov, V.; Kumar, N.; Lemeshko, S.; Li, J.-F.; Luszcz, K.; Maleki, T.; Meixner, A. J.; Minne, S.; Raschke, M. B.; Ren, B.; Rogalski, J.; Roy, D.; Stephanidis, B.; Wang, X.; Zhang, D.; Zhong, J.-H.; Zenobi, R. *J. Raman Spectrosc.* **2014**, *45*, 22.
(49) Timofeir, S.; Kurunczi, L.; Schmidt, W.; Simon, Z. *SAR QSAR Environ. Res.* **2002**, *13*, 219.
(50) Leona, M.; Casadio, F.; Bacci, M.; Picollo, M. *J. Am. Inst. Conserv.* **2004**, *43*, 37.
(51) Deckert-Gaudig, T.; Deckert, V. *J. Raman Spectrosc.* **2009**, *40*, 1446.
(52) Sonntag, M. D.; Chulhai, D.; Seiderman, T.; Jensen, L.; Van Duyne, R. P. *J. Am. Chem. Soc.* **2013**, *135*, 17187.
(53) Klingsporn, J. M.; Sonntag, M. D.; Seideman, T.; Van Duyne, R. P. *J. Phys. Chem. Lett.* **2014**, *5*, 106.
(54) Wang, H.; Schultz, Z. D. *Analyst* **2013**, *138*, 3150.
(55) Kizil, R.; Irudayaraj, J.; Seetharaman, K. *J. Agric. Food Chem.* **2002**, *50*, 3912.
(56) Zannini, P.; Baraldi, P.; Aceto, M.; Agostino, A.; Fenoglio, G.; Bersani, D.; Canobbio, E.; Schiavon, E.; Zanichelli, G.; De Pasquale, A. *J. Raman Spectrosc.* **2011**, *43*, 1722.
(57) Hahn, O.; Kanngiesser, B.; Malzer, W. *Stud. Conserv.* **2005**, *50*, 23.
(58) Wagner, B.; Bulska, E. *J. Anal. At. Spectrom.* **2004**, *19*, 1325.
(59) Bardon, T.; May, R. K.; Taday, P. F.; Strlic, M. *Analyst* **2013**, *138*, 4859.
(60) Lee, A. S.; Mahon, P. J.; Creagh, D. C. *Vib. Spectrosc.* **2006**, *41*, 170.
(61) Deckert-Gaudig, T.; Deckert, V. *Small* **2009**, *5*, 432.
(62) Blum, C.; Schmidt, T.; Opilik, L.; Weidmann, S.; Fagerer, S. R.; Zenobi, R. *J. Raman Spectrosc.* **2012**, *43*, 1895.
(63) Kazemi-Zanjani, N.; Chen, H.; Goldberg, H. A.; Hunter, G. K.; Grohe, B.; Lagugne-Labarthet, F. *J. Am. Chem. Soc.* **2012**, *134*, 17076.
(64) Rasmussen, A.; Deckert, V. *J. Raman Spectrosc.* **2006**, *37*, 311.
(65) Mohammed-Ziegler, I.; Billes, F. *J. Mol. Struct.* **2002**, *618*, 259.